Monthly Notices
of the
ROYAL ASTRONOMICAL SOCIETY

Mon. Not. R. Astron. Soc. **418,** 1156–1164 (2011) doi:10.1111/j.1365-2966.2011.19567.x

Discovery of a stripped red giant core in a bright eclipsing binary system⋆

P. F. L. Maxted,[1]† D. R. Anderson,[1] M. R. Burleigh,[2] A. Collier Cameron,[3] U. Heber,[4] B. T. Gänsicke,[5] S. Geier,[4] T. Kupfer,[4] T. R. Marsh,[5] G. Nelemans,[6] S. J. O'Toole,[7] R. H. Østensen,[8] B. Smalley[1] and R. G. West[2]

[1]*Astrophysics Group, Keele University, Keele, Staffordshire ST5 5BG*
[2]*Department of Physics and Astronomy, University of Leicester, University Road, Leicester LE1 7RH*
[3]*SUPA, School of Physics and Astronomy, University of St. Andrews, North Haugh, Fife KY16 9SS*
[4]*Dr Karl Remeis-Observatory & ECAP, Astronomical Institute, Friedrich-Alexander University Erlangen-Nuremberg, Sternwartstr. 7, D 96049 Bamberg, Germany*
[5]*Department of Physics, University of Warwick, Coventry CV4 7AL*
[6]*Department of Astrophysics, IMAPP, Radboud University Nijmegen, PO Box 9010, 6500 GL Nijmegen, the Netherlands*
[7]*Australian Astronomical Observatory, PO Box 296, Epping, NSW 1710, Australia*
[8]*Institute of Astronomy, K.U. Leuven, Celestijnenlaan 200D, 3001 Heverlee, Belgium*

Accepted 2011 August 2. Received 2011 July 29; in original form 2011 June 28

ABSTRACT

We have identified a star in the Wide Angle Search for Planets (WASP) archive photometry with an unusual light curve due to the total eclipse of a small, hot star by an apparently normal A-type star and with an orbital period of only 0.668 d. From an analysis of the WASP light curve together with V-band and I_C-band photometry of the eclipse and a spectroscopic orbit for the A-type star we estimate that the companion star has a mass of $0.23 \pm 0.03\,M_\odot$ and a radius of $0.33 \pm 0.01\,R_\odot$, assuming that the A-type star is a main-sequence star with the metallicity appropriate for a thick-disc star. The effective temperature of the companion is $13\,400 \pm 1200$ K from which we infer a luminosity of $3 \pm 1\,L_\odot$. From a comparison of these parameters to various models we conclude that the companion is most likely to be the remnant of a red giant star that has been very recently stripped of its outer layers by mass transfer on to the A-type star. In this scenario, the companion is currently in a shell hydrogen-burning phase of its evolution, evolving at nearly constant luminosity to hotter effective temperatures prior to ceasing hydrogen burning and fading to become a low-mass white dwarf composed of helium (He-WD). The system will then resemble the pre-He-WD/He-WD companions to A- and B-type stars recently identified from their *Kepler* satellite light curves (KOI-74, KOI-81 and KIC 10657664). This newly discovered binary offers the opportunity to study the evolution of a stripped red giant star through the pre-He-WD stage in great detail.

Key words: binaries: close – binaries: eclipsing – binaries: spectroscopic – stars: individual: 1SWASP J024743.37−251549.2 – stars: peculiar.

1 INTRODUCTION

Wide-area surveys for transiting extrasolar planets such as Wide Angle Search for Planets (WASP; Pollacco et al. 2006), Hungarian Automated Telescope Network (HATnet; Bakos et al. 2004), XO (McCullough et al. 2005) and Trans-atlantic Exoplanet Survey (TrES; O'Donovan, Charbonneau & Hillenbrand 2006) provide high cadence photometry for millions of bright stars across a large fraction of the sky. This provides the opportunity to find and study many new examples of known classes of variable star, e.g. eclipsing brown dwarf binary systems (Anderson et al. 2011), double-mode RR Lyr stars (Wils 2010), W UMa stars (Norton et al. 2011), young solar-type stars (Messina et al. 2011) and cataclysmic variable stars (Wils 2011). New discoveries will certainly be made now that much of the data from these surveys is becoming widely available (Butters et al. 2010). The photometric precision achieved by these surveys with modest equipment ($\lesssim$0.01 mag at $V \approx 12$) is

⋆Based on observations made with ESO Telescopes at the La Silla Observatory under programme ID 084.D-0348(A).
†E-mail: pflm@astro.keele.ac.uk

impressive, but cannot compete with the micromagnitude photometry achieved from space by surveys such as *Convection Rotation and planetary Transits* (*CoRoT*; Baglin et al. 2006) and *Kepler* (Borucki et al. 2009). Photometry with this precision has made it possible to identify new types of variable star that are difficult or impossible to study from the ground, e.g. triply eclipsing binary stars (Carter et al. 2011b), stars with tidally excited pulsations (Welsh et al. 2011), subdwarfs with white dwarf companions (Bloemen et al. 2011) and white dwarf companions to early-type main-sequence stars (Rowe et al. 2010; van Kerkwijk et al. 2010).

One advantage that ground-based surveys currently have over space-based surveys is that they cover a much larger fraction of the sky. This makes is possible in some cases to discover rare or extreme examples of these new classes of variable star. In the case of the white dwarf companions to early-type stars KOI-74 and KOI-81, these were identified from the eclipses and transits in the *Kepler* light curves, even though these features are much less than 1 per cent deep (Rowe et al. 2010; van Kerkwijk et al. 2010). These low-mass white dwarfs have an unusual evolutionary history, but it is difficult to study them in detail because they are very much fainter than their companions. Ground-based surveys offer the opportunity to discover similar eclipsing binary systems that are more favourable for detailed follow-up observations.

Low-mass white dwarf stars ($M < 0.4\,\mathrm{M}_{\odot}$) are the product of binary star evolution (Iben & Livio 1993; Marsh, Dhillon & Duck 1995). They are the result of mass transfer from a red giant on to a companion star when the giant has a small degenerate helium core. There are several possible outcomes from this mass transfer depending on the mass ratio of the binary and the type of companion star. If the companion is a neutron star then the mass transfer is likely to stable so the binary can go on to become a low-mass X-ray binary (LMXB) containing a millisecond pulsar. Several millisecond radio pulsars are observed to have low-mass white dwarf (LMWD) companions (Lorimer 2008). Many new LMWDs have recently been identified in the Sloan Digital Sky Survey (SDSS; Kilic et al. 2007) and from proper motion surveys (Kawka & Vennes 2009). Searches for radio pulsar companions to these LMWDs have so far found nothing, suggesting that the majority of these LMWDs have white dwarf companions (Agüeros et al. 2009). LMWD can also be produced by mass transfer from a red giant on to a main-sequence star, either rapidly through unstable common-envelope evolution or after a longer lived 'Algol' phase of stable mass transfer (Refsdal & Weigert 1969; Giannone & Giannuzzi 1970; Iben & Livio 1993; Nelson & Eggleton 2001; Chen & Han 2003; Willems & Kolb 2004).

The evolution of LMWDs is expected to be very different from more massive white dwarfs. It is expected that once mass transfer stops the LMWD will have a thick layer of hydrogen surrounding the degenerate helium core which leads to steady hydrogen shell burning via the p–p chain and can lead to unstable phases of CNO burning for LMWD in the mass range 0.2–0.3 $\mathrm{M}_{\odot}$ (Driebe et al. 1999). These hydrogen shell flashes lead to mixing between the inner and outer layers, producing a hydrogen deficient surface composition for the LMWD. Models that include hydrogen shell burning provide a much better match between the 'cooling age' of the LMWD and the 'spin-down age' of the millisecond pulsars in LMXBs. The number of hydrogen shell flashes depends strongly on the mass of the hydrogen layer that remains on the surface of the LMWD (Sarna, Ergma & Gerškevitš-Antipova 2000), which in-turn depends strongly on the details of the mass loss from the red giant (Podsiadlowski, Rappaport & Pfahl 2002). Details such as the treatment of diffusion can also lead to large differences in the predictions between different models (Althaus, Serenelli & Benvenuto 2001).

In this paper we present the discovery from WASP photometry of an eclipsing binary star that is related to KOI-74, KOI-81 but that has much deeper eclipses, i.e. the companion to the early-type star is much brighter and larger than the white dwarf companions to these *Kepler* discoveries. We present the data used to identify this new eclipsing binary star and the follow-up photometry and spectroscopy we have obtained; we analyse these data to determine the masses, radii and luminosities of the stars and we outline how our discovery of this bright pre-white dwarf companion to an early-type star makes it possible to study the formation of an LMWD in detail.

2 OBSERVATIONS AND DATA REDUCTION

2.1 WASP photometry

The star 1SWASP J024743.37−251549.2 (hereafter J0247−25) was observed by the WASP-South instrument as part of the WASP survey. The WASP survey is described in Pollacco et al. (2006) and Wilson et al. (2008). The data from this survey are automatically processed and analysed in order to identify stars with light curves that contain transit-like features that may indicate the presence of a planetary companion. The candidate selection methods can be found in Collier Cameron et al. (2007), Pollacco et al. (2008) and references therein. In practice, these automatic methods produce tens of thousands of candidates, so we use a data base to store the results of the automatic analysis plus other information available for the stars such as catalogue photometry and astrometry. This makes it possible to efficiently reject large numbers of candidates that are unlikely to host planets using a variety of criteria such as eclipse depth and the noise level in the light curve. The number of candidates that remain after sifting is small enough to make selection by inspection of the available data by a small number of people feasible. The same data base can also be used to identify eclipsing binary stars by modifying the sifting criteria.

J0247−25 was spotted by one of us (PFLM) while looking at light curves of stars with deep eclipses and low reduced proper motions, i.e. stars that may be eclipsing binary subdwarfs. Catalogue photometry and astrometry of J0247−25 are summarized in Table 1. The automatic transit detection algorithm correctly identified a period of 0.6678 d from 6633 observations of this star obtained with the WASP-South instrument. The observations were obtained with a single camera through a broad-band filter (400–700 nm) between 2006 August 10 and 2007 December 31. The WASP photometry is shown as a function of orbital phase in Fig. 1. The deeper of the two eclipses in the light curve shows a flat section between a sharp ingress and egress. This type of light curve is produced by the eclipse of one star by a larger but cooler star. It is not possible to produce a light curve with these properties if both the stars in the binary are on the main sequence. For this reason we organized follow-up observations of this unusual object.

2.2 SAAO 1.0-m photometry

We observed the egress phases of two eclipses of J0247−25 using the University of Cape Town (UCT) CCD photometer on the South African Astronomical Observatory (SAAO) 1.0-m telescope. The star approximately 2.5 mag fainter located 71 arcsec west of

Table 1. Catalogue photometry and astrometry of J0247−25. *The Galaxy Evolution Explorer* (*GALEX*) far-ultraviolet (FUV) and near-ultraviolet (NUV) fluxes are given as AB magnitudes $f_{\rm AB}$ and $n_{\rm AB}$, respectively. Sources are *GALEX* (Morrissey et al. 2007), Naval Observatory Merged Astrometric Dataset (NOMAD; Zacharias et al. 2004) PPMXL (Roeser, Demleitner & Schilbach 2010), third USNO CCD Astrograph Catalog (UCAC3; Zacharias et al. 2010) and Two Micron All Sky Survey (2MASS; Skrutskie et al. 2006).

Parameter	Value	Source
RA (J2000.0)	02 47 43.38	NOMAD
Dec. (J2000.0)	−25 15 49.3	NOMAD
μ_α	23.2 ± 2.5 mas yr^{-1}	PPMXL
	25.9 ± 1.2 mas yr^{-1}	UCAC3
μ_δ	-5.4 ± 1.2 mas yr^{-1}	PPMXL
	-5.3 ± 1.0 mas yr^{-1}	UCAC3
$f_{\rm AB}$	16.03 ± 0.02	*GALEX*
$n_{\rm AB}$	14.46 ± 0.01	*GALEX*
B	12.13	NOMAD
V	12.44	NOMAD
J	11.85	2MASS
H	11.81	2MASS
$K_{\rm s}$	11.79	2MASS

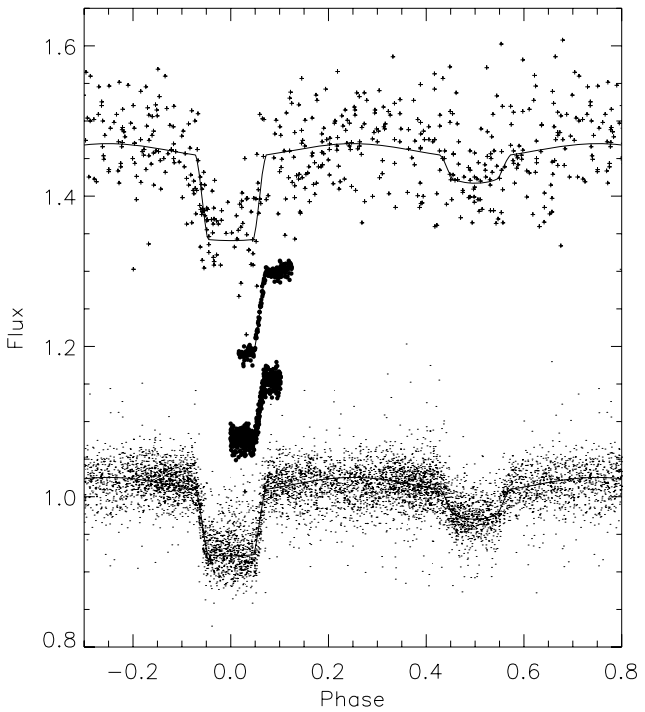

Figure 1. Light curves of J0247−25 with light-curve model fits (solid lines). From bottom to top: WASP (small points); SAAO 1.0-m $I_{\rm C}$- and V band (filled circles); ASAS V band (small crosses).

J0247−25 was used as a comparison star. Images with an exposure time of 10 s through an $I_{\rm C}$-band filter were obtained on the night 2009 October 30. Exposures with an exposure time of 30 s through a V-band filter were obtained on the night 2009 November 5. We used synthetic aperture photometry to measure the apparent fluxes of J0247−25 and the comparison star. The apparent flux of J0247−25 relative to the comparison star normalized to the flux out of eclipse is shown in Fig. 1.

2.3 Spectroscopy

We obtained nine spectra of J0247−25 on four nights with the Gemini Multi-Object Spectrographs (GMOS) on the Gemini-South telescope using the 600 line mm^{-1} grating and a 0.5-arcsec slit. We only used the data from the CCD covering the wavelength range 3698–4619 Å for this study. The resolution of these spectra estimated from a Gaussian fit to an arc line is approximately 2.5 Å and the dispersion is 0.9 Å pixel^{-1}. We also obtained six spectra with the ESO Faint Object Spectrograph and Camera 2 (EFOSC2) spectrograph on the ESO New Technology Telescope (NTT) with grism #19. These spectra cover the wavelength range 4434–5109 Å at a dispersion of 0.67 Å pixel^{-1} and have a resolution of approximately 2.2 Å. Finally, we obtained two consecutive spectra of J0247−25 with the Intermediate dispersion Spectrograph and Imaging System (ISIS) spectrograph on the 4.2-m William Herschel Telescope (WHT). These spectra cover the wavelength range 3984–4776 Å at a dispersion of 0.22 Å pixel^{-1} and have a resolution of 0.6 Å.

3 ANALYSIS

We refer to the larger, cooler component of J0247−25 as J0247−25 A and its companion (the star eclipsed at phase 0) as J0247−25 B.

3.1 Light-curve model

In addition to the three light curves we obtained, we also analysed the V-band photometry for J0247−25 provided by the All Sky Automated Survey (ASAS; Pojmanski 2002). We used only the 503 measurements graded 'A' for our analysis. We used the light-curve model EBOP (Etzel 1981; Popper & Etzel 1981) to analyse all four light curves simultaneously and so derive the following parameters: the radii of the stars relative to their separation, $R_{\rm A}/a$ and $R_{\rm B}/a$; the inclination, i; the ratio of the surface brightnesses for the stars at each wavelength, $S_{\rm WASP}$, $S_{\rm ASAS}$, S_V and $S_{I_{\rm C}}$; the linear limb-darkening coefficients in the V- and $I_{\rm C}$-band, x_V and $x_{I_{\rm C}}$, respectively; the time (HJD UTC) of mid-primary eclipse, T_0; the orbital period, P and the normalization of the four light curves. For the WASP data we use the average of x_V and $x_{I_{\rm C}}$ as the linear limb-darkening parameter. We assigned the same linear limb-darkening coefficient to both stars because the limb darkening of J0247−25 B has a negligible effect on the light curve. For numerical stability and to avoid non-physical values for the various parameters, the free parameters we use in the least-squares fit are following: $\log(S_{\rm WASP})$; $\log(S_{\rm ASAS})$; $\log(S_V)$; $\log(S_{I_{\rm C}})$; $\log(1/b - 1)$ (where $b = a\cos i/[R_{\rm A} + R_{\rm B}]$ is the impact parameter); $R_{\rm A}/a$; $k = R_{\rm B}/R_{\rm A}$; $(P - 0.66783173) \times 1000$; $T_0 - 245\,5134.6272$; $\log(1/x_V - 1)$; $\log(1/x_{I_{\rm C}} - 1)$; $\log(q)$ (where $q = M_{\rm B}/m_{\rm A}$ is the mass ratio). The optimum values of the parameters of interest derived by least squares are given in Table 2. The standard errors on the parameters are derived used a bootstrap Monte Carlo method. The fits to the light curves can be seen in Fig. 1. The joint distributions from the Monte Carlo simulation for selected pairs of parameters are shown in Fig. 2. The linear limb-darkening parameters x_V and $x_{I_{\rm C}}$ are found to be indeterminate from the light curve and the other parameters have only a weak dependence on them.

Table 2. Parameters for the light-curve model fit by least squares. Parameter definitions are given in the text.

Parameter	Value
T_0	245 5135.29504 ± 0.00004
P (d)	0.6678321 ± 0.0000002
$S_{\rm ASAS}$	3.36 ± 0.16
$S_{\rm WASP}$	2.50 ± 0.14
S_I	2.16 ± 0.12
S_V	3.17 ± 0.15
b	0.163 ± 0.007
$R_{\rm A}/a$	0.4492 ± 0.0025
$R_{\rm B}/a$	0.0866 ± 0.0023
k	0.1929 ± 0.0043
q	0.121 ± 0.005
i (°)	85.0 ± 0.2

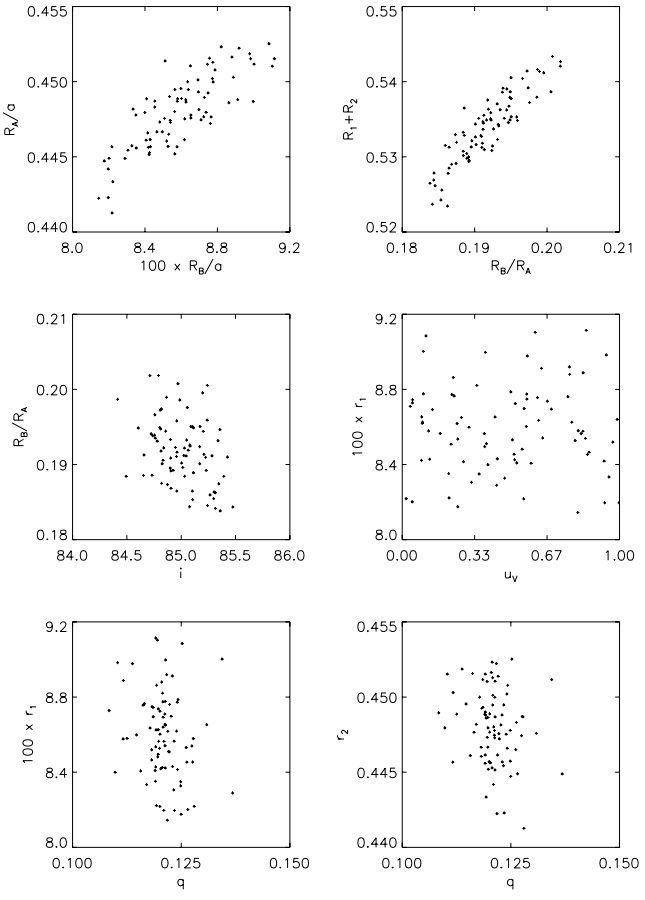

Figure 2. Distribution of selected light-curve parameters from the bootstrap Monte Carlo simulation.

3.2 Effective temperatures of J0247−25 A and J0247−25 B

We used the observed $V - K$ colour of J0247−25 combined with the luminosity ratio and surface brightness ratio in the V band from the light-curve solution to estimate the effective temperatures of J0247−25 A and J0247−25 B. For the V-band magnitude we used the mean value of V from the ASAS photometry, with the sample standard deviation as a standard error, 12.28 ± 0.07. This standard error is intended to account for the variation of the flux between eclipses and any systematic offset from the ASAS V band and the standard V-band photometric system. We use the observed value of $K_{\rm s}$ from Table 1 but as the phase at which this magnitude was measured is not known we assign it the same standard error as the sample standard deviation of the WASP photometry. We also convert the $K_{\rm s}$ magnitude to K using $(K_{\rm s})_{\rm 2MASS} = K - 0.044$ (Bessell 2005) to obtain $K = 11.83 \pm 0.05$.

The effective temperature of a single star with $V - K = 0.45$ is 8250 K (Zombeck 2007). We used the spectral energy distributions from Kurucz (1993) to calibrate the relation between surface brightness and effective temperature in the V band. We then used the initial value of $T_{\rm eff,A} = 8400$ K for J0247−25 A and the values of S_V from the light-curve solution to obtain $T_{\rm eff,B} = 14\,050$ K for J0247−25 B. We then use the $V - K$ value for a star of this effective temperature and the luminosity ratio in the V band from the light-curve solution to derive a value of $(V - K)_{\rm A} = 0.51 \pm 0.09$. Repeating the steps above then leads to the improved effective temperature estimates of $T_{\rm eff,A} = 8060 \pm 330$ K for J0247−25 A and $T_{\rm eff,B} = 13\,400 \pm 1200$ K for J0247−25 B.

We did not attempt a detailed analysis of our spectra for J0247−25 because we were not able to clearly identify any spectral lines from J0247−25 B. This makes it very difficult to account for the contamination of the combined spectrum by J0247−25 B, particularly since this highly evolved star may have a very peculiar atmospheric composition, e.g. it may be hydrogen deficient. We were able to estimate that the projected rotational velocity of J0247−25 A is $V_{\rm A} \sin i = 95 \pm 5\,{\rm km\,s^{-1}}$ from the observed widths of various metal lines.

3.3 Spectroscopic orbit of J0247−25 A

The flux-calibrated spectrum of J0247-25 is compared to the spectrum of the A6Vp star HD148898 in Fig. 3. We measured the radial velocity of J0247−25 A by cross-correlation of the spectra against a high-resolution spectrum of HD 148898 (Bagnulo et al. 2003). We excluded the broad Balmer lines from the cross-correlation. There is no indication of a second peak in the cross-correlation function due to J0247−25 B. The radial velocities derived from the cross-correlation function are given in Table 3. These radial velocities have been corrected for the radial velocity of the template star (2.5 km s^{-1}; Wilson 1953). For well-exposed spectra such as these the dominant sources of error are systematic, e.g. motion of the

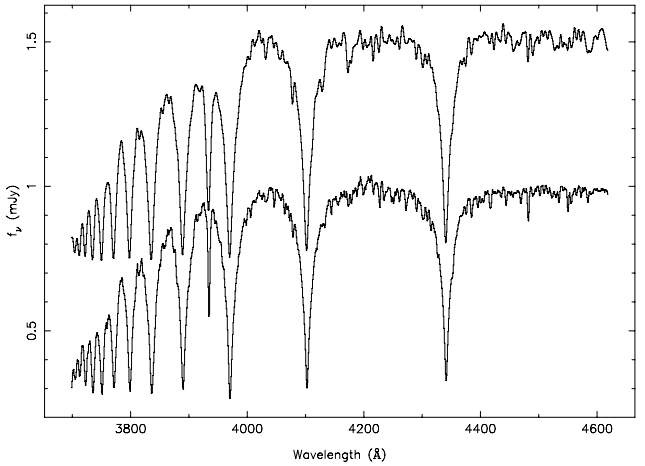

Figure 3. Flux calibrated and normalized GMOS-S spectrum of J0247−25 (lower spectrum) compared to the normalized, flux calibrated and smoothed spectrum of the A6Vp star HD 148898 offset by +0.5 units (upper spectrum).

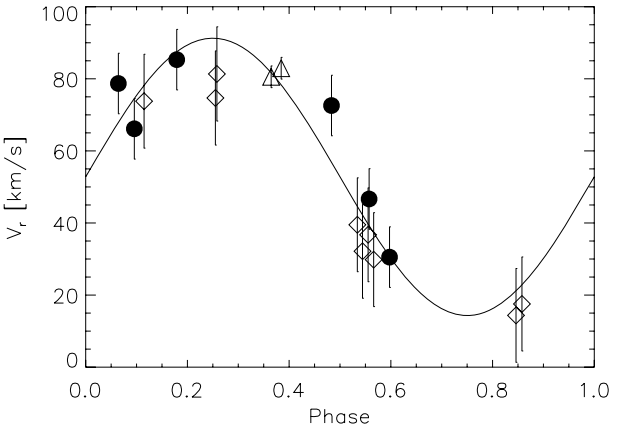

Figure 4. Radial velocity measurements of J0247−25 B as a function of phase with a circular orbit fit (solid line). The spectrograph used is indicated as follows: filled circles – EFOSC2; triangles – ISIS; diamonds – GMOS.

Table 3. Heliocentric radial velocities for J0247−25 A.

HJD −245 0000	V_r (km s^{-1})	Instrument
5137.5367	80.5 ± 3.0	ISIS
5137.5499	82.9 ± 3.0	ISIS
5144.6820	78.7 ± 8.4	EFOSC2
5144.7587	85.3 ± 8.4	EFOSC2
5145.6794	46.6 ± 8.4	EFOSC2
5145.7060	30.5 ± 8.4	EFOSC2
5146.7065	66.1 ± 8.4	EFOSC2
5147.6335	72.5 ± 8.4	EFOSC2
5128.6879	74 ± 13	GMOS-S
5129.8440	14 ± 13	GMOS-S
5129.8522	18 ± 13	GMOS-S
5130.7851	75 ± 13	GMOS-S
5130.7873	81 ± 13	GMOS-S
5141.6567	40 ± 13	GMOS-S
5141.6638	32 ± 13	GMOS-S
5141.6709	37 ± 13	GMOS-S
5141.6780	30 ± 13	GMOS-S

Table 4. Circular orbit fit for J0247−25 A. The function fitted to the radial velocities in Table 3 from $\gamma + K_A \sin[2\pi(\mathrm{HJD} - T_0)/P]$.

Parameter	Value	
T_0	245 5135.295	(fixed)
P (d)	0.66783	(fixed)
γ (km s^{-1})	52.6	± 2.4
K_A (km s^{-1})	38.5	± 3.6
N	17	
χ^2	12.2	

star in the slit and instrument flexure. From experience we find that using dispersion/5 gives a reasonable estimate of the standard error in these cases, so this is the value given in Table 3.

The parameters of the spectroscopic orbit assuming zero eccentricity in the least-squares fit are given in Table 4 and the results are shown in Fig. 4.

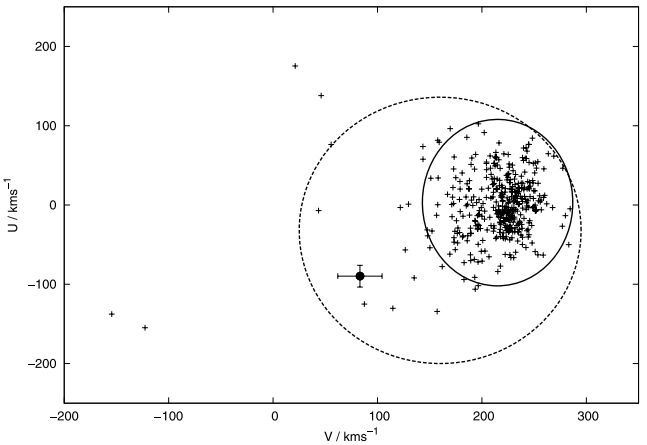

Figure 5. Galactic U–V velocities for J0247−25 (error bar) compared to the sample of white dwarfs from Pauli et al. (2006). The contours define the 3σ ellipse for thin disc (full drawn) and thick disc (dashed) stars as defined by Pauli et al.

3.4 Kinematics

We have calculated the Galactic U–V velocity components of J0247−25 using the method described by Pauli et al. (2003). We used the mean of the proper motion values given in Table 1 and assigned an error of 1.5 mas to each component. The radial velocity of the system is taken from Table 4. We used the isochrones from Siess, Dufour & Forestini (2000) to estimate that a zero-age main-sequence star with the same effective temperature as J0247−25 A has an absolute V magnitude $M_V = 1.4 \pm 0.3$. We calculated the apparent V magnitude of J0247−25 A assuming that it contributes 89 per cent of the light in the V band. From the apparent distance modulus of J0247−25 A and ignoring the effects of reddening we estimate the distance to J0247−25 to be $d = 1500 \pm 300$ pc. The resulting U–V velocity components for J0247−25 are shown in Fig. 5 compared to the region of this diagram occupied by thin-disc and thick-disc stars. J0247−25 clearly has the kinematics of a thick-disc star, which suggests that it is likely to be old ($\gtrsim$7 Gyr), metal poor ($-1 \lesssim$ [Fe/H] $\lesssim -0.3$) and have enhanced α-element abundance ([Mg/Fe] $\gtrsim 0.3$).

3.5 Mass, radius and luminosity of the components

Using Kepler's third law we find that the density of J0247−25 A, ρ_A, is related to the orbital period, the parameter R_A/a derived from the light-curve model and the mass ratio, $q = M_B/M_A$, as follows:

$$\rho_A = \frac{3\pi}{G(1+q)(R_A/a)^3 P^2}. \quad (1)$$

The value of ρ_A is not sensitive to the exact value of q provided this value is small, so we take a value of $q = 0.16 \pm 0.08$ and compare the values of ρ_A and $T_{\mathrm{eff,A}}$ to the stellar models for main-sequence stars from Girardi et al. (2000). This value of q is chosen for consistency with the masses derived below. The error on q is arbitrary but large enough to easily cover all likely values for this parameter. For the models shown in Fig. 6 the best estimate of the mass is $1.48 \pm 0.09\,\mathrm{M}_\odot$ where the error includes the uncertainties in $T_{\mathrm{eff,A}}$, ρ_A and [Fe/H] $= -0.65 \pm 0.35$.

In Table 5 we give the values for the mass, radius and luminosity for J0247−25 A and J0247−25 B derived from the light-curve model and mass function assuming $M_A = 1.48 \pm 0.09\,\mathrm{M}_\odot$.

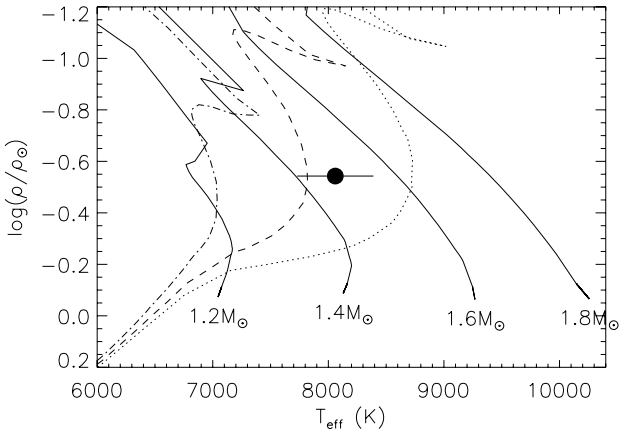

Figure 6. The effective temperature and density of J0247−25 A compared to the models of Girardi et al. (2000) for $Z = 0.004$. Stellar evolutionary tracks are shown as thick lines and labelled by mass. Isochrones for log (age/Gyr) = 9.0, 9.2 and 9.4 are plotted with dotted, dashed and dash–dotted lines, respectively.

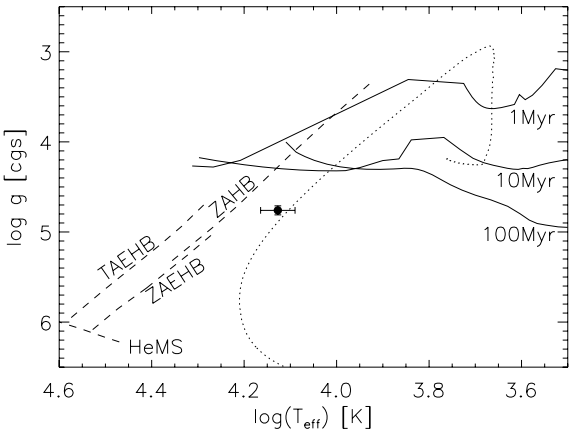

Figure 7. The effective temperature and surface gravity of J0247−25 B compared to the models for core hydrogen burning stars (solid lines), core helium burning stars (dashed lines) and a model for the formation of a 0.195 $M_\odot$ white dwarf (dotted line; Driebe et al. 1999). Core hydrogen burning models from Siess et al. (2000) are labelled by age. Core helium burning models are labelled as follows: ZAEHB/TAEHB = zero-age/terminal-age extreme horizontal branch (Dorman, Rood & O'Connell 1993); ZAHB = zero-age horizontal branch (Sweigart 1987); HeMS = helium main sequence (Dorman et al. 1993).

Table 5. Physical parameters of the components of J0247−25.

Parameter	J0247−25 A	J0247−25 B
Mass ($M_\odot$)	1.48 ± 0.09^a	0.23 ± 0.03^a
Radius ($R_\odot$)	1.71 ± 0.04^a	0.33 ± 0.01^a
$T_{\rm eff}$ (K)	8060 ± 330	$13\,400 \pm 1200$
log g (cgs)	4.13 ± 0.02^a	4.75 ± 0.05
Luminosity ($L_\odot$)	11 ± 2^a	3 ± 1^a

[a]Assuming J0247−25 A is a main-sequence star with [Fe/H] = −0.65 ± 0.35.

4 DISCUSSION

Our estimate of the surface gravity for J0247−25 B, $\log g_{\rm B}$, is independent of the assumed mass for J0247−25 A (Southworth et al. 2004) so in Fig. 7 we compare the observed values of $T_{\rm eff,B}$ and $\log g_{\rm B}$ to various models. It is clear that J0247−25 B cannot be a core hydrogen-burning star and is too cool to be a core helium-burning star. In contrast, the model for the formation of a 0.195 $M_\odot$ white dwarf from Driebe et al. (1999) is a good match to the observed values of $T_{\rm eff,B}$ $\log g_{\rm B}$ and a reasonable match to the estimated value of $M_{\rm B}$. We therefore conclude that J0247−25 B is the precursor of a low-mass white dwarf. As this white dwarf will be composed almost entirely of helium, we refer to J0247−25 B and similar stars as pre-He-WD stars.

In Fig. 8 we show the Hertzsprung–Russell diagram (HRD) for various models of the formation of low-mass white dwarfs and the observed positions of J0247−25 B and some related objects. The objects KOI-74 and KOI-81 discussed earlier appear to form an evolutionary sequence with J0247−25 B according to these models, with KOI-81 coming towards the end of the pre-He-WD phase and KOI-74 being near the start of the white dwarf cooling track. KIC 10657664 is a companion to an A-type star also identified from *Kepler* photometry (Carter, Rappaport & Fabrycky 2011a). The *Kepler* light curve of this binary shows a well defined total eclipse approximately 2 per cent deep, a secondary eclipse and variations between the eclipses that were identified as the Doppler beaming (DB) signal due to the orbital motion of the A-type star and the ellipsoidal variation (ELV) due to its tidal deformation. The mass ratio for the binary can be estimated from either the DB or ELV

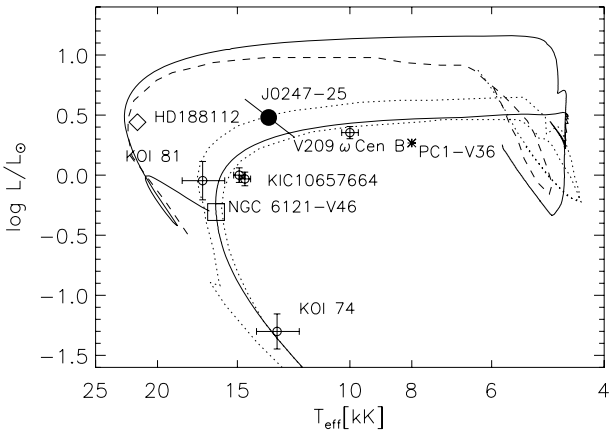

Figure 8. J0247−25 B in the HRD (filled circle). Other objects discussed in the text are also plotted. Models for the formation of low-mass white dwarfs (with final masses as noted, bottom to top) are also shown as follows: Driebe et al. (1999) – solid lines (0.195 and 0.234 $M_\odot$); Nelson, Dubeau & MacCannell (2004) – dotted lines (0.205 and 0.215 $M_\odot$); van Kerkwijk et al. (2010) – dashed lines (0.21 $M_\odot$).

signal, but these are found to be inconsistent with one another unless the A-type star has a mass much lower than expected (0.7 $M_\odot$ cf. 2.5 $M_\odot$). HD 188112 is a single-lined spectroscopic binary star for which the mass ($0.24^{+0.10}_{-0.07}$ $M_\odot$) can be inferred from its *Hipparcos* parallax (Heber et al. 2003). The companion to this star is a compact object and the orbital of the system 0.606585 d. The object PC1-V36 is a binary star with an orbital period of 0.8 d in the globular cluster 47 Tuc (Knigge et al. 2008). The companion to this very low mass object ($M = 0.056\,M_\odot$) is very faint and may be a neutron star. NGC 6121-V46 is also a binary star in a globular cluster (M4) with an unseen companion (O'Toole et al. 2006).

The object V209 ω Cen B is one component of an eclipsing binary with a period of 0.83 d in the globular cluster ω Cen (Kaluzny et al. 2007). This star also has a similar mass to J0247−25 B (0.144 ± 0.008 $M_\odot$). The other component in this binary star, V209 ω Cen A,

is too hot to be a main-sequence star given its mass ($T_{\rm eff}$= 9370 K, $M = 0.945\,{\rm M}_{\odot}$). This casts doubt on our assumption that the mass of J0247−25 A can be estimated from models of normal main-sequence stars. The same doubt applies to the analysis of KIC 10657664 by Carter et al. (2011a), who also assumed that the A-type primary star in that binary is a main-sequence star because a mass of $0.8\,{\rm M}_{\odot}$ for a star with $T_{\rm eff} \approx 9500$ K is 'not physically plausible'. Kaluzny et al. suggest that V209 ω Cen A may be a white dwarf that has accumulated sufficient mass to re-ignite shell hydrogen burning. As far as we can ascertain, this intriguing scenario has not been studied further.

The position of J0247−25 B in Fig. 7 is not affected by the assumed mass for J0247−25 A, so an alternative way to estimate the mass of J0247−25 A is to assume that J0247−25 B has a mass of $0.195\,{\rm M}_{\odot}$ from the model of Driebe et al. (1999) that is a good match to the observed values of $T_{\rm eff,B}$ and $\log g_{\rm B}$. In this case, the mass function implies a mass of $M_{\rm A} = 1.2 \pm 0.2\,{\rm M}_{\odot}$, i.e. similar to the mass of V209 ω Cen A. Alternatively, if we assume that J0247−25 A rotates synchronously, then the observed value of $V_{\rm A} \sin i = 95 \pm 5\,{\rm km\,s^{-1}}$ combined with the parameters in Table 2 can be used to infer the value of the semimajor axis, a, and thus $M_{\rm A} \approx 0.6\,{\rm M}_{\odot}$ and $M_{\rm B} \approx 0.13\,{\rm M}_{\odot}$. Finally, we can use the mass ratio estimated from the light-curve solution together with the mass function to estimate $M_{\rm A} = 2.8 \pm 1.0\,{\rm M}_{\odot}$. This estimate must be regarded with some caution because the only feature of the light curve that depends strongly on q is the ellipsoidal variation in brightness between eclipses. It is not known at the time writing whether the algorithm used to remove systematic noise from the WASP light curves may also reduce the strength of variations on time-scales of ∼8 h, i.e. the duration of observations on a typical night and the period of the ellipsoidal variation in J0247−25. Although these various estimates of $M_{\rm A}$ are not consistent with one another, this does not affect our main conclusion that J0247−25 B is a pre-He-WD.

We have not shown in Fig. 8 the complex evolutionary paths followed by low-mass white dwarfs during hydrogen shell flashes. Some of these paths match the observed properties of J0247−25 B rather well, but the time-scale for the evolution through the relevant part of the HRD is generally extremely short (decades–centuries), so this is a rather remote possibility.

J0247−25 B contributes about 11 per cent of the flux at visible wavelengths so better quality spectroscopy should make it possible to directly measure the radial velocity of J0247−25 B and so derive precise, model-independent masses for both stars. It will also be possible to recover the individual spectra of the two components of J0247−25 by comparing the spectra in-eclipse and out-of-eclipse or using spectral disentangling techniques (Pavlovski & Hensberge 2010). This will make it possible to test the prediction of Driebe et al. (1999) that a $0.195\,{\rm M}_{\odot}$ white dwarf should have a helium-enhanced atmosphere at this stage of its evolution as a consequence of the extreme mass loss that this star has suffered.

Models for the formation of LMWD suggest that the relationship between orbital period and white dwarf mass ($P_{\rm b}$–$M_{\rm WD}$ relation) should be almost independent of the details of how the mass is lost from the red giant, although the relation is expected to show some dependence on metallicity. In practice, these models seem to underestimate the mass of LMWD companions to millisecond pulsars (Stairs et al. 2005). The masses and periods of various low-mass white dwarf and pre-He-WD binary systems are given in Table 6 and are compared to selected models for their formation through a phase of stable mass transfer in Fig. 9. The relation between mass and period is very steep at the short-period end, so precise and accurate (model independent) mass measurements

Table 6. Masses and periods for low-mass white dwarfs and pre-He-WDs in binary systems.

Name	Period (d)	Mass ($\rm M_{\odot}$)	Source
NGC 6121-V46	0.087	∼0.19	1
HD 188112	0.607	$0.24^{+0.10}_{-0.07}$	2
J0247−25	0.668	0.23 ± 0.03	3
PC1-V36	0.794	0.056 ± 0.018	4, 5
V209 ω Cen B	0.834	0.144 ± 0.008	6
KIC 10657664	3.274	0.26 ± 0.04	7
		0.37 ± 0.08	7
KOI-74	5.189	0.22 ± 0.03	8
KOI-81	23.89	∼0.3	8
Regulus B	40.11	0.30 ± 0.02	9

Note. References: 1 – O'Toole et al. (2006); 2 – Heber et al. (2003); 3 – this paper; 4 – Albrow et al. (2001); 5 – Kaluzny et al. (2007); 6 – Kaluzny et al. (2007); 7 – Carter et al. (2011a); 8 – van Kerkwijk et al. (2010); 9 – Rappaport, Podsiadlowski & Horev (2009).

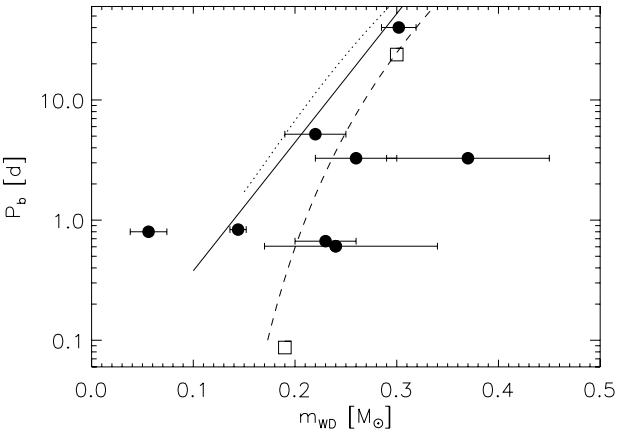

Figure 9. The masses and periods for low-mass white dwarfs and pre-He-WDs from Table 6 compared to selected models as follows: solid line – Nelson et al. (2004); dotted line – Rappaport et al. (1995); dashed line – Tauris & Savonije (1999). Star for which the mass estimates have no quoted error bar is shown with open symbols.

are needed to define an empirical $P_{\rm b}$–$M_{\rm WD}$ relation. Spectroscopy of J0247−25 with sufficient signal-to-noise ratio and resolution to allow a spectroscopic orbit for J0247−25 B to be measured should yield a precise mass estimate for J0247−25 B. This would make possible an interesting comparison with V209 ω Cen B and PC1-V36, which have similar orbital periods to J0247−25 but that are both members of metal-poor globular clusters.

It seems clear that the formation of J0247−25 must have involved extensive mass loss from a red giant star, but the mechanism for the mass loss is not so clear. The progenitor of J0247−25 B must have had a mass $\gtrsim 0.8\,{\rm M}_{\odot}$ to evolve off the main sequence within the lifetime of the Galaxy, so this star has lost $\gtrsim 0.5\,{\rm M}_{\odot}$. This suggests that J0247−25 B has accreted rather a lot of material or the evolution of this binary system has required highly non-conservative mass transfer. A full exploration of the possible evolutionary pathways for the formation of J0247−25 is beyond the scope of this paper, but we note here that the low projected rotational velocity of J0247−25 A may be a very useful constraint in any such study. If the mass of J0247−25 B is $\gtrsim 0.2\,{\rm M}_{\odot}$ then J0247−25 A must be rotating subsynchronously or have significantly non-zero obliquity. This would be difficult to explain in any scenario in which J0247−25 A

has gained a large amount of mass and angular momentum from the red giant progenitor to J0247−25 B. Nevertheless, J0247−25 A appears to be a young star when compared to the isochrones for metal-poor stars shown in Fig. 6 (1–2 Gyr), certainly much younger than a typical star in the thick-disc population (Feltzing & Bensby 2008). This suggests that J0247−25 A has gained enough mass from its companion to become a blue straggler, i.e. an anomalously young, massive star when compared to other thick-disc stars. The synchronization time-scale for a 1.4 $M_\odot$ star is about 10 Myr (Claret 2004), comparable to the time since the formation of J0247−25 B according to the 0.195 $M_\odot$ model of Driebe et al. (1999). This suggests that there has not been sufficient time for J0247−25 A to have lost a large amount of rotational angular momentum through tidal interactions with J0247−25 B since its formation. It may be that the formation of J0247−25 B left J0247−25 A far from equilibrium and that the slow rotation is caused by the subsequent expansion of this star.

5 CONCLUSIONS

The star 1SWASP J024743.37−251549.2 is an eclipsing binary star in which the precursor to a low-mass white dwarf with a mass $\approx$0.25 $M_\odot$ is totally eclipsed by a larger, cooler star once every 0.6678 d. More detailed spectroscopy will be required to measure a precise mass for the stars. This will enable us to determine the nature of the larger star and to make detailed tests of models for the formation pre-He-WDs and low-mass white dwarfs.

ACKNOWLEDGMENTS

Funding for WASP comes from consortium universities and from the UK Science and Technology Facilities Council.

WASP-South is hosted by the South African Astronomical Observatory and we are grateful for their ongoing support and assistance.

This publication makes use of data products from the Two Micron All Sky Survey, which is a joint project of the University of Massachusetts and the Infrared Processing and Analysis Center/California Institute of Technology, funded by the National Aeronautics and Space Administration and the National Science Foundation.

Based on observations obtained at the Gemini Observatory, which is operated by the Association of Universities for Research in Astronomy, Inc., under a cooperative agreement with the NSF on behalf of the Gemini partnership: the National Science Foundation (USA), the Science and Technology Facilities Council (UK), the National Research Council (Canada), CONICYT (Chile), the Australian Research Council (Australia), Ministério da Ciência e Tecnologia (Brazil) and Ministerio de Ciencia, Tecnología e Innovación Productiva (Argentina) (Program ID GS-2009B-Q-96).

REFERENCES

Agüeros M. A., Camilo F., Silvestri N. M., Kleinman S. J., Anderson S. F., Liebert J. W., 2009, ApJ, 697, 283
Albrow M. D., Gilliland R. L., Brown T. M., Edmonds P. D., Guhathakurta P., Sarajedini A., 2001, ApJ, 559, 1060
Althaus L. G., Serenelli A. M., Benvenuto O. G., 2001, MNRAS, 323, 471
Anderson D. R. et al., 2011, ApJ, 726, L19
Baglin A., Auvergne M., Barge P., Deleuil M., Catala C., Michel E., Weiss W., The COROT Team, 2006, in Fridlund M., Baglin A., Lochard J., Conroy L., eds, ESA Special Publication Vol. 1306, Scientific Objectives for a Minisat: CoRoT. ESA, Noordwijk, p. 33
Bagnulo S., Jehin E., Ledoux C., Cabanac R., Melo C., Gilmozzi R., The ESO Paranal Science Operations Team, 2003, Messenger, 114, 10
Bakos G., Noyes R. W., Kovács G., Stanek K. Z., Sasselov D. D., Domsa I., 2004, PASP, 116, 266
Bessell M. S., 2005, ARA&A, 43, 293
Bloemen S. et al., 2011, MNRAS, 410, 1787
Borucki W. et al., 2009, in Pont F., Sasselov D., Holman M., eds, Proc. IAU Symp. 253, KEPLER: Search for Earth-Size Planets in the Habitable Zone. Cambridge Univ. Press, Cambridge, p. 289
Butters O. W. et al., 2010, A&A, 520, L10
Carter J. A., Rappaport S., Fabrycky D., 2011a, ApJ, 728, 139
Carter J. A. et al., 2011b, Sci, 331, 562
Chen X., Han Z., 2003, MNRAS, 341, 662
Claret A., 2004, A&A, 424, 919
Collier Cameron A. et al., 2007, MNRAS, 380, 1230
Dorman B., Rood R. T., O'Connell R. W., 1993, ApJ, 419, 596
Driebe T., Blöcker T., Schönberner D., Herwig F., 1999, A&A, 350, 89
Etzel P. B., 1981, in Carling E. B., Kopal Z., eds, Photometric and Spectroscopic Binary Systems. Reidel, Dordrecht, p. 111
Feltzing S., Bensby T., 2008, Phys. Scr. T, 133, 014031
Giannone P., Giannuzzi M. A., 1970, A&A, 6, 309
Girardi L., Bressan A., Bertelli G., Chiosi C., 2000, A&AS, 141, 371
Heber U., Edelmann H., Lisker T., Napiwotzki R., 2003, A&A, 411, L477
Iben I., Jr, Livio M., 1993, PASP, 105, 1373
Kaluzny J., Rucinski S. M., Thompson I. B., Pych W., Krzeminski W., 2007, AJ, 133, 2457
Kawka A., Vennes S., 2009, A&A, 506, L25
Kilic M., Allende Prieto C., Brown W. R., Koester D., 2007, ApJ, 660, 1451
Knigge C., Dieball A., Maíz Apellániz J., Long K. S., Zurek D. R., Shara M. M., 2008, ApJ, 683, 1006
Kurucz R., 1993, ATLAS9 Stellar Atmosphere Programs and 2 km/s grid. Kurucz CD-ROM No. 13. Smithsonian Astrophysical Observatory, Cambridge, MA
Lorimer D. R., 2008, Living Rev. Relativ., 11, 8
McCullough P. R., Stys J. E., Valenti J. A., Fleming S. W., Janes K. A., Heasley J. N., 2005, PASP, 117, 783
Marsh T. R., Dhillon V. S., Duck S. R., 1995, MNRAS, 275, 828
Messina S., Desidera S., Lanzafame A. C., Turatto M., Guinan E. F., 2011, A&A, 532, A10
Morrissey P. et al., 2007, ApJS, 173, 682
Nelson C. A., Eggleton P. P., 2001, ApJ, 552, 664
Nelson L. A., Dubeau E., MacCannell K. A., 2004, ApJ, 616, 1124
Norton A. J. et al., 2011, A&A, 528, A90
O'Donovan F. T., Charbonneau D., Hillenbrand L., 2006, BAAS, 38, 1212
O'Toole S. J., Napiwotzki R., Heber U., Drechsel H., Frandsen S., Grundahl F., Bruntt H., 2006, Baltic Astron., 15, 61
Pauli E.-M., Napiwotzki R., Altmann M., Heber U., Odenkirchen M., Kerber F., 2003, A&A, 400, 877
Pauli E.-M., Napiwotzki R., Heber U., Altmann M., Odenkirchen M., 2006, A&A, 447, 173
Pavlovski K., Hensberge H., 2010, in Prša A., Zejda M., eds, ASP Conf. Ser. Vol. 435, Reconstruction and Analysis of Component Spectra of Binary and Multiple Stars. Astron. Soc. Pac., San Francisco, p. 207
Podsiadlowski P., Rappaport S., Pfahl E. D., 2002, ApJ, 565, 1107
Pojmanski G., 2002, Acta Astron., 52, 397
Pollacco D. L. et al., 2006, PASP, 118, 1407
Pollacco D. et al., 2008, MNRAS, 385, 1576
Popper D. M., Etzel P. B., 1981, AJ, 86, 102
Rappaport S., Podsiadlowski P., Joss P. C., Di Stefano R., Han Z., 1995, MNRAS, 273, 731
Rappaport S., Podsiadlowski P., Horev I., 2009, ApJ, 698, 666
Refsdal S., Weigert A., 1969, A&A, 1, 167
Roeser S., Demleitner M., Schilbach E., 2010, AJ, 139, 2440
Rowe J. F. et al., 2010, ApJ, 713, L150
Sarna M. J., Ergma E., Gerškevitš-Antipova J., 2000, MNRAS, 316, 84
Siess L., Dufour E., Forestini M., 2000, A&A, 358, 593
Skrutskie M. F. et al., 2006, AJ, 131, 1163

Southworth J., Zucker S., Maxted P. F. L., Smalley B., 2004, MNRAS, 355, 986
Stairs I. H. et al., 2005, ApJ, 632, 1060
Sweigart A. V., 1987, ApJS, 65, 95
Tauris T. M., Savonije G. J., 1999, A&A, 350, 928
van Kerkwijk M. H., Rappaport S. A., Breton R. P., Justham S., Podsiadlowski P., Han Z., 2010, ApJ, 715, 51
Welsh W. F. et al., 2011, ApJ, submitted (arXiv:1102.1730)
Willems B., Kolb U., 2004, A&A, 419, 1057
Wils P., 2010, Inf. Bull. Var. Stars, 5955, 1
Wils P., 2011, J. American Association Var. Star Obser., 39, 60
Wilson R. E., 1953, General Catalogue of Stellar Radial Velocities. Carnegie Institution, Washington
Wilson D. M. et al., 2008, ApJ, 675, L113
Zacharias N., Monet D. G., Levine S. E., Urban S. E., Gaume R., Wycoff G. L., 2004, BAAS, 36, 1418
Zacharias N. et al., 2010, AJ, 139, 2184
Zombeck M., 2007, Handbook of Space Astronomy and Astrophysics, 3rd edn. Cambridge Univ. Press, Cambridge

This paper has been typeset from a TEX/LATEX file prepared by the author.